# Phosphatic nodules from the Early Miocene Kamenoo Formation near Nakoso, Jōban Coal Field, Japan

Kazuhiko KANO*

**Abstract :** Phosphatic nodules, including $P_2O_5$ of 8–16 wt%, were newly found in porcellaneous rocks at an outcrop of the Early Miocene Kamenoo Formation. Phosphate in the nodules is a modification of fluorapatite, presumably carbonate-fluorapatite, and forms cocoon-shaped or oval minute grains of submicroscopic size. Phosphate content increases with decreasing silica toward the center of the nodules. Judging from the sedimentological and petrological features, the host rocks are diatomaceous oozes in origin, which were deposited on continental shelf or slope not so far from land and at the level of the oxygen minimum zone. Authigenic silica minerals in the nodules, host rocks and other associated rocks show that the nodules were formed in the early stage of diagenesis. Consequently, it is very likely that the phosphatic nodules are genetically similar to those in recent diatomaceous oozes on the sea floor.

## Introduction

Since early times, phospatic rocks in marine sediments have attracted much attention of geologists and geochemists because of the limited occurrence in sediment piles and extraordinarily high concentration of a biophile element, phosphorous. However, examples of marine phosphatic rocks described in Japan are not so many ; they occur as concretions in Paleozoic limestone (INOUE, 1964), Permian shale (KANISAWA and EHIRO, 1986) and Neogene shallow-marine sediments (TSUNETO, 1897; KAMOSHITA, 1898; ŌTSUKA, 1900; HAMACHI, 1962 ; OGIWARA and TAGUCHI, 1986), as thin layers in cherts of Sambosan Belt (MATSUBARA *et al.*, 1985) and as lenticular or massive deposits in Miocene shallow-marine sediments (IMAI and YAMADA, 1952; MORITANI,1967). In

this connection, this paper describes phosphatic nodules newly found from the marine siliceous rocks of the Early Miocene Kamenoo Formation.

## Geologic setting

The Kamenoo Formation is a formation of the Early to Middle Miocene Yunagawa Group extensively distributed in the coastal region of Fukushima Prefecture and northern-most of Ibaraki Prefecture, and represents the deepest facies of a marine transgression-regression cycle of the Group (SUGAI *et al.*, 1957). The formation amounting up to 150 m in thickness is characteristically composed of finely laminated and/or bedded siliceous to siliceous argillaceous rocks with shale, siltstone, sandstone and acidic tuff. Slump beds and sandstone turbidites are found frequently (IWAI, 1953). Carbonate concretions, some of which are somewhat rich in phosphorus, are occasionally present (HIRABAYA-

---

*   Geology Department

SHI, 1977). Many constituent rocks include brownish moss-green biotite flakes, probably derived from the Abukuma metamorphic rocks cropping out behind the coastal region. Siliceous fossils, mainly of diatoms and sponge spicules, are common. In addition, molds of molluscs such as *Acila eximia, Yoldia tokunagai* and *Lucinoma kamenooensis*, fossils of broad leaves, and debris of a mammal, *desmostylus mirabilis* have been reported (SUGAI *et al.*, 1957). The lithologic and paleontologic features suggest that the depositional environment of the Kamenoo Formation was continental shelf or slope not so far from land.

### Mode of occurrence

Phosphatic nodules were found in the typical sequence of the Kamenoo Formation at an outcrop near Nakoso (Figs. 1 and 2). The sequence, 45 m in thickness, occupies the middle part of the formation and is composed mainly of porcellanite to porcellaneous shale, diatomaceous shale and diatomaceous siltstone. Porcellanite, porcellaneous shale and diatomaceous shale have fine parallel laminae with variable thickness less than 5 mm, and are more or less friable except porcellanite. On the other hand, diatomaceous siltstone appears massive, but is bioturbated and shows microscopically visible discontinuous parallel or sub-parallel laminae. The siliceous to siliceous argillaceous rocks are brownish grey to dark brown in color.

Phosphatic nodules occur in porcellaneous rocks at two horizons of the sequence (Fig. 2). The nodules are yellowish light grey to yellowish white, and earthy or as soft as diatomite. The nodule surface is somewhat irregular but does not have any broken features, and cannot be defined sharp. Laminae are visible in the nodules and can be traced to the host rocks, indicating that the nodules replaced the host sediments. An example of the nodules is shown in Plate I.

### Experimental methods

13 samples of phosphatic nodules and siliceous to siliceous argillaceous rocks were collected from the sequence (Fig. 2). and examined chemically and mineralogi-
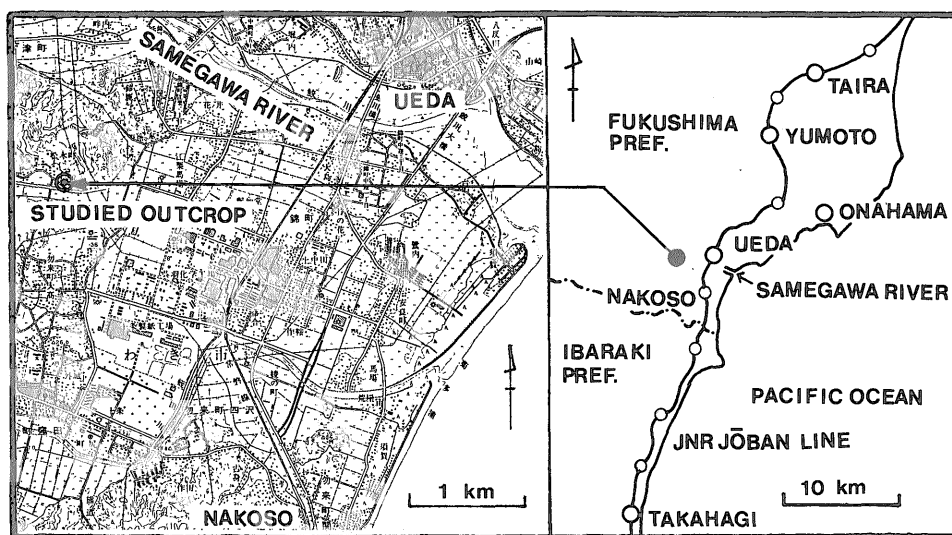


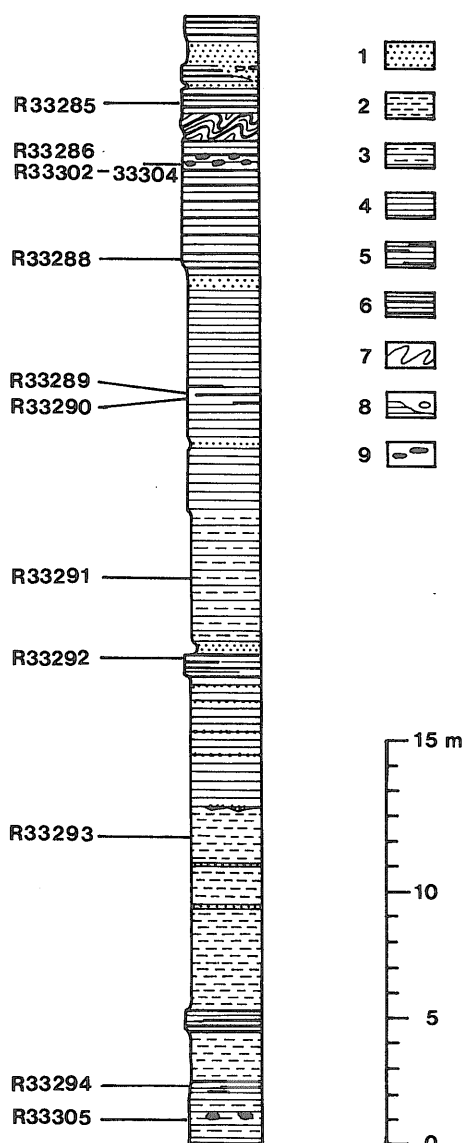Fig. 1 Locality of the outcrop where phosphatic nodules were found.

Fig. 2  Sedimentary sequence at the outcrop shown in Fig. 1.

1:sandstone, 2:diatomaceous siltstone, 3:diatomaceous shale with thin layers of sandstone and/or siltstone, 4:diatomaceous shale, 5:diatomaceous shale with porcellaneous lenses, 6:alternation of porcellaneous shale and porcellanite partly with diatomaceous shale, 7:slump bed, 8:erosion and clasts, 9:phosphatic nodule. Numerals on the left side of this figure are of samples collected and registered as the Geological Museum Samples of Geological Survey of Japan.

cally.

Minerals were identified principally through the X-ray diffractometry, and the relative content of minerals were estimated according to the heights of characteristic peaks of the minerals on the X-ray diffractograms of bulk samples. The d-spacings of apatite and the d (101) spacing of opal-CT were measured, referring to low quartz as an internal standard. The measurement error of the d (101) spacing of opal-CT was $\pm 0.05$ A. The cell parameters $a_0$ and $c_0$ of apatite were calculated with the error of 0.001 A by using a least-square method. In the calculation, weak and/or broad diffraction lines which make the error of calculated cell parameters larger were eliminated.

The chemical compositions of bulk samples were determined through the X-ray fluorescence analysis. For the analysis, samples were heated at 1000°C for 1 hour and weighed the loss on ignition. Subsequently, the sample were mixed with lithium-tetraborate so as to be 1 : 10 in weight ratio. Samples with high phosphorous content were diluted by mixing with pure silica before heating at 1000°C. In this case, the weight ratio of original sample to pure silica was about 1 : 10, so that the measurement error is estimated to be about 10 times as large as that of other samples.

Some samples were dissolved by using warm 6N HCl solution, and fluorine dissolved in the solution was quantitatively determined by using an ion-selective electrode. Fluorine determined through this method was probably derived from only phosphate minerals.

### Experimental results

#### (1)  Chemical compositions

Phosphatic nodules contain $P_2O_5$ of 8–16 wt% and CaO of 9–17 wt%, and the weight

ratio $CaO/P_2O_5$ are very close to that of apatite (Fig. 3). $SiO_2$ is also a major chemical component. MnO, MgO and $Na_2O$ are detected a little, but one phosphatic nodule contains a significant amount of MnO, reaching about 2 wt%. The chemical compositions of representative samples are shown in Table 1.

On the other hand, porcellanite and porcellaneous shale contain $SiO_2$ of 76–90 wt%, and diatomaceous shale and siltstone of 70–76 wt%, respectively on ignition loss-free basis. $P_2O_5$ in these rocks are 0.2 wt% in most cases. In porcellaneous

rocks at the phosphate-bearing horizons, it is however somewhat high, 0.2–0.9 wt% and increases up to 4 wt% in very close proximity to the phosphatic nodules.

Notable is an inverse relation between $P_2O_5$ and $SiO_2$ contents in phosphatic nodules and phosphate-bearing host rocks (Fig. 4). A detailed examination of the content profiles of $P_2O_5$ and $SiO_2$ along a cross section from host rock to phosphatic nodule indicates that $P_2O_5$ increases as $SiO_2$ decreases toward the phosphatic nodule (Fig. 5). This relation may result from the replacement of silica by phos-
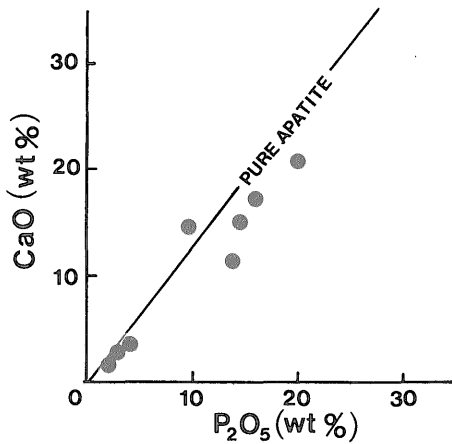


Fig. 3  The relation of $P_2O_5$ to CaO in the bulk samples of phosphatic nodules and phosphate-bearing host rocks.
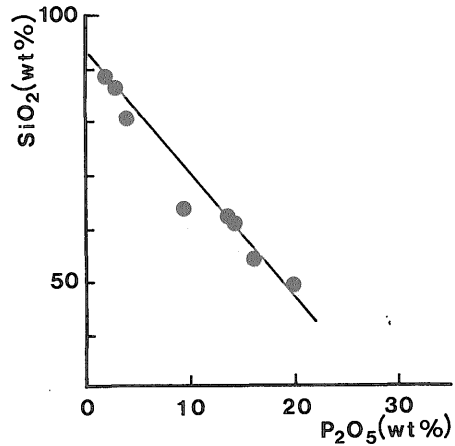


Fig. 4  The relation of $P_2O_5$ to $SiO_2$ in the bulk samples of phosphatic nodules and phosphate-bearing host rocks.
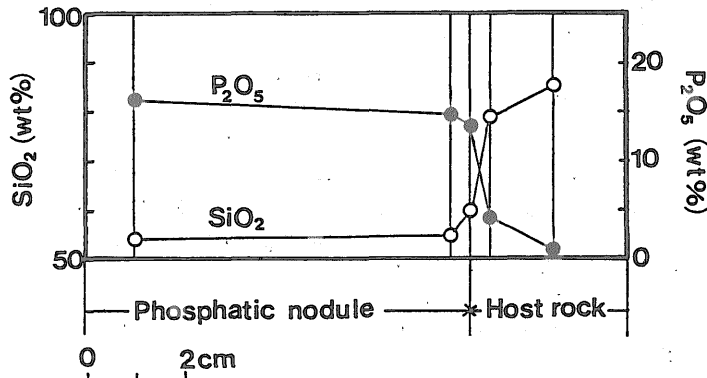


Fig. 5  Content profiles of $P_2O_5$ and $SiO_2$ along a cross section from the center of phosphatic nodule R33286 to the host rock.

Table 1   Chemical compositions of representative phosphatic nodules.

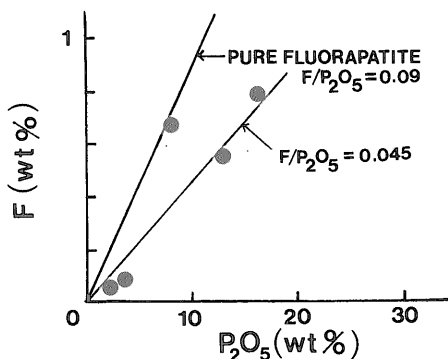| Sample | B 33286–1 | R 33303 |
|---|---|---|
| $SiO_2$ | 46. 7 | 40. 2 |
| $TiO_2$ | 0. 6 | 0. 7 |
| $Al_2O_3$ | 4. 7 | 6. 4 |
| $Fe_2O_3$* | 4. 2 | 2. 0 |
| MnO | tr. | tr. |
| MgO | tr. | tr. |
| CaO | 14. 8 | 17. 1 |
| $Na_2O$ | tr. | tr. |
| $K_2O$ | 0. 6 | 0. 3 |
| $P_2O_5$ | 13. 7 | 16. 4 |
| Ig. loss | 13. 2 | 17. 3 |
| Total | 98. 5 | 100. 4 |
| F** | n. d. | 0. 79 |

* : total Fe as $Fe_2O_3$.
** : determined by H. GOTO through the method described in the text.
tr. : trace. n. d. : not determined.



Fig. 6   The relation of $P_2O_5$ to F in the bulk samples of phosphatic nodules and phosphate-bearing host rocks.

phate.

### (2)   Constituent minerals

The major constituent minerals in phosphatic nodules are apatite, opal-CT and/ or opal-A. On the other hand, diatom frustules and sponge spicules made of opal-A are common in diatomaceous rocks, and their molds transformed to opal-CT in porcellaneous rocks. Opal-CT in both phosphatic nodules and porcellaneous rocks are 4.11–4.10 Å in the d (101) spacing. Some porcellaneous rocks, particularly in close proximity to phosphatic nodules, include a little amount of apatite. Silt-sized grains of quartz, feldspars and moss-green biotite, smectite and framboidal pyrite are ubiquitous in phosphatic nodules, and porcellaneous and diatomaceous rocks. Glauconite, and molds of foraminiferal tests replaced by silica are recognized sporadically in porcellaneous and diatomaceous rocks. Minor amounts of clinoptilolite, calcite and gypsum are rarely found in diatomaceous rocks. Gypsum forms veinlets cutting the laminae and is lined with hematitic mineral, suggesting that it is a products under aerobic conditions presumably near the earth-surface.

Apatite in the phosphate-bearing samples resembles fluoroapatite in the X-ray diffraction pattern (Table 2). The weight ratio $F/P_2O_5$ in the samples ranges from 0.045 to 0.09, suggesting that the molar ratio of fluorine in the apatite is 0.5–1 (Fig. 6). However, the cell parameter $a_0$ is somewhat less than that of fluorapatite (Table 2). The $a_0$ normally decreases in the order, chlorapatite, hydroxyapatite, fluorapatite and carbonate-fluorapatite and /or carbonate-hydroxyapatite (*cf.* DEER *et al.*, 1962, and see also Fig. 7). This, combined with the above lines of evidence, allow us to interpret the apatite as a modification of fluorapatite, presumably carbonate-fluorapatite. According to the X-ray diffraction method of GULBRANDSEN (1970), the $CO_2$ content in the apatite is estimated to be in the range from 3 to 5 wt%.

The apatite forms generally cryptocrystalline cocoon-shaped or oval grains smaller than 3 $\mu$m (Plate II). The energy-dispersive X-ray spectrographs of the

Table 2   X-ray diffraction data of apatites.

| (1) | | | (2) | | (3) | | (4) | |
|---|---|---|---|---|---|---|---|---|
| d(A) | I/I₁ | hkl | d(A) | I/I₁ | d(A) | I/I₁ | d(A) | I/I₁ |
| 8.12 | 8 | 100 | 8.09 | 9 | 8.09 | 5 | 8.09 | 6 |
| 5.25 | 4 | 101 | 5.25 | 4 | 5.29 | 4 | 5.25 | 3 |
| 4.684 | 1 | 110 | | | | | | |
| 4.055 | 8 | 200 | P | | P | | P | |
| 3.872 | 8 | 111 | 3.869 | 8 | 3.875 | 8 | 3.868 | 7 |
| 3.494 | 1 | 201 | | | | | | |
| 3.442 | 40 | 002 | 3.444 | 45 | 3.446 | 42 | 3.454 | 43 |
| 3.167 | 14 | 102 | P | | P | | P | |
| 3.067 | 18 | 210 | 3.059 | 12 | 3.059 | 18 | 3.060 | 16 |
| 2.800 | 100 | 211 | 2.794 | 100 | 2.796 | 100 | 2.794 | 100 |
| 2.772 | 55 | 112 | 2.769** | 60 | 2.769** | 58 | 2.769** | 50 |
| 2.702 | 60 | 300 | 2.698* | 46 | 2.699* | 45 | 2.695* | 47 |
| 2.624 | 30 | 202 | 2.623* | 24 | 2.623* | 19 | 2.625* | 29 |
| 2.517 | 6 | 301 | 2.505 | 12 | 2.509* | 7 | 2.514* | 11 |
| 2.289 | 8 | 212 | 2.281 | 14 | 2.283 | 11 | 2.284 | 16 |
| 2.250 | 20 | 310 | 2.243* | 22 | 2.243* | 21 | 2.241* | 25 |
| 2.218 | 4 | 221 | 2.215 | 4 | 2.218 | 5 | 2.214 | 5 |
| 2.140 | 6 | 311 | 2.139 | 6 | 2.141 | 6 | | |
| 2.128 | 4 | 302 | 2.127 | 13 | 2.127 | 10 | 2.129 | 14 |
| 2.061 | 6 | 113 | 2.059* | 6 | 2.058 | 5 | 2.064* | 9 |
| 2.028 | 2 | 400 | 2.026 | 2 | 2.024 | 2 | | |
| 1.997 | 4 | 203 | 1.996 | 7 | 2.000 | 4 | 1.997 | 8 |
| 1.937 | 25 | 222 | 1.932* | 22 | 1.934* | 21 | 1.933* | 25 |
| 1.884 | 14 | 312 | 1.880 | 11 | 1.881 | 11 | 1.879 | 13 |
| 1.862 | 4 | 320 | | | | | | |
| 1.837 | 30 | 213 | 1.836* | 29 | 1.838* | 28 | 1.838* | 29 |
| 1.797 | 16 | 321 | 1.792* | 11 | 1.794* | 12 | 1.791* | 13 |
| 1.771 | 14 | 410 | 1.766* | 10 | 1.767* | 11 | 1.764* | 10 |
| 1.748 | 14 | 402 | 1.745* | 12 | 1.746* | 10 | 1.746* | 12 |
| 1.722 | 16 | 004 | 1.723* | 16 | 1.724* | 13 | 1.724* | 13 |
| 1.684 | 1 | 104 | | | | | | |
| 1.637 | 6 | 322 | 1.635 | 4 | 1.635 | 6 | 1.634 | 5 |
| 1.607 | 4 | 313 | 1.605 | 4 | 1.607 | 4 | | |

| a₀ = 9.3684 | a₀ = 9.342 A | a₀ = 9.348 A | a₀ = 9.335 A |
|---|---|---|---|
| c₀ = 6.8841 A | c₀ = 6.888 A | c₀ = 6.899 A | c₀ = 6.899 A |

(1) Fluorapatite (ASTM 15-876),  (2) R 33286-1,  (3) R 33303 and (4) R 33305.
* : line used to compute the cell parameters a₀ and c₀.
** : line recognized as a shoulder of the line (211).
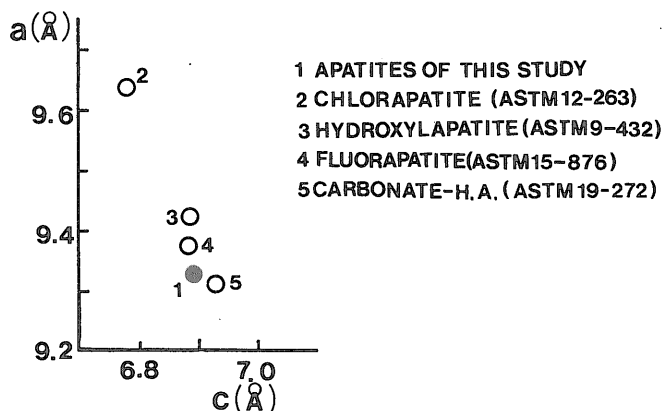P : line masked by other lines of opal-CT and feldspars.

Fig. 7   The relation of the cell parameters $a_0$ and $c_0$ and the types
of apatite.

grains indicate the presence of phosphorus and calcium with minor amounts of silicon and aluminum (Plate II). Silicon and aluminum in the grains may be impurities.

## Discussions

1)   Phosphatic nodules described here are undoubtedly of diagenetic origin. The host porcellaneous rocks have reached an incipient stage of opal-A to opal-CT transformation, while opal-A in associated diatomaceous rocks remains almost unchanged. Therefore, referring to the silica mineral changes (*cf*. MIZUTANI, 1970, 1977; ISAACS, 1982; KANO, 1983), it is likely that the phosphatic nodules were formed in the earliest stage of silica mineral diagenesis.

2)   The host porcellaneous rocks include abundant molds of diatom frustules, and are therefore diatomaceous oozes in origin.   They were deposited probably on continental shelf or slope not so far from land, as suggested already.   In recent marine environments, finely parallel-laminated diatomaceous oozes are found to be dominant at the level of the oxygen minimum zone while massive diatomaceous oozes may occur above and below the oxygen minimum zone (INGLE, 1981; PISCI-

OTTO and GARRISON, 1981).   This implies that the sequence of finely parallel-laminated and massive diatomaceous rocks (and/or porcellaneous rocks of diatomaceous ooze-origin) such as that studied here may have been deposited in and around the depths of the oxygen minimum zone.   The oxygen minimum zone, if present, is below the euphotic zone (shallower than 80 m normally), and likely to be in the depths of continental shelf to slope.

3)   The above discussions allow us to suppose that the phosphatic nodules in question were formed in diatomaceous oozes on continental shelf or slope which were in contact with the oxygen minimum zone.   According to the recent reviews by BENTOR (1980) and BATURIN (1982), phosphatic nodules are formed near the sediment-water interface, and most of recent phosphatic nodules are found in diatomaceous oozes on continental shelf. The phosphate-producing oozes face the oxygen minimum zone and are underlain by upwelling sea water with high biological productivity.   Thus, the oozes are usually rich in organic matter, which is oxidized by sulfate-reducing bacteria under anaerobic conditions and releases the constituent biophile elements into the interstitial water.   As a result, phosphate

is precipitated probably at the pH of 7.0–7.4. In that process, phosphate often replaces silica of the oozes. This story of precipitation process of marine phosphate is widely accepted, and would be applicable to the present case.

## Conclusions

1) Phosphatic nodules occur in finely parallel-laminated porcellaneous rocks in the diatomaceous sequence of the Miocene Kamenoo Formation, that were probably deposited on continental shelf or slope not so far from land and faced the oxygen minimum zone.

2) The nodules include $P_2O_5$ of 8–16 wt% and CaO of 9–17 wt%, most of which form loosely-packed cocoon-shaped or oval grains of apatite less than 3 $\mu$m in diameter.

3) They were formed through replacing silica, presumably when the original sediments were below or near the sea floor.

### References

BATURIN, G. N. (1982) *Phosphorites on the Sea Floor*. Elsevier, 343 p.

BENTOR, Y. K. (1980) Phosphorites —— the unsolved problems. *Soc. Econ. Paleontol. Mineral.*

*Spec. Publ.*, no. 29, p. 3–18.

DEER, W. A., HOWIE, R. A. and ZUSSMAN, J. (1962) Apatites. in *Rock–Forming Minerals*, vol. 5, p. 323–338.

GULBRANDSEN, R. A. (1970) Relation of carbon dioxide content of apatite of the Phosphoria Formation to regional facies. *U. S. Geol. Surv. Prof. Pap.* 700B, p. 9–13.

HAMACHI, T. (1962) On the uraniferous nodules at Nakajō-machi, Kitakambara-gun, Niigata Prefecture. *Bull. Geol. Surv. Japan*, vol. 13, p. 583–588 (in Japanese with English abstract).

HIRABAYASHI, K. (1977) Sedimentological and geochemical study of carbonate concretions in the Jōban Coal–Field and Oga Peninsula. *Sci. Rep. Tohoku Univ.*, Ser. 3, vol. 13, p. 183–226.

IMAI, H. and YAMADA, H. (1952) The peculiar phophate deposits in the Noto Peninsula, Japan. *Jour. Geol. Soc. Japan*, vol. 58, p. 79–93.

INGLE, J. C. Jr. (1981) Origin of the Neogene diatomites around the North Pacific rim. in *The Monterey Formation and Related Siliceous Rocks of California*, Soc. Econ. Paleontol. Mineral., Pacific Section, p. 159–179.

INOUE, H. (1964) Apatite in the Tsukumi Limestone, Oita Prefecture. *Sekkaiseki* (*Limestone*), no. 90, p. 434–439 (in Japanese).

ISAACS, C. M. (1982) Influence of rock composition on kinetics of silica phase changes in the Monterey Formation, Santa Barbara area, California. *Geology*, vol. 10, p. 304–308.

IWAI, J. (1953) Interformational abnormal deposition observed in the Kameno-o Formation. *Contrib. Inst. Geol. Paleontol. Tohoku Univ.*, no. 42, p. 1–22 (in Japanese).

KAMOSHITA, M. (1898) Report on the investigation of phosphate beds in Yamamoto Province, Ugo and in Mogami Province, Uzen. *Bull. Imperial Geol. Surv. Japan*, vol. 12, no. 2, p. 103–118 (in Japanese).

KANISAWA, S. and EHIRO, M. (1986) Occurrence and geochemical nature of phosphatic rocks and Mn-rich carbonate rocks in the Toyoman Series, Kitakami Mountains, northeastern Japan. *Jour. Japan. Assoc. Mineral Petrol. Econ. Geol.*, vol. 81, p. 12–31.

KANO, K. (1983) Ordering of opal-CT in diagene-

sis. *Geochem. Jour.*, vol. 17, p. 87–93.

MATSUBARA, S., SAITO, Y. and KATO, A. (1985) Phosphate minerals in cherts of the Sambosan Belt (abstract). *Jour. Japan. Assoc. Mineral. Petrol. Econ. Geol.*, vol. 80, p. 159 (in Japanese).

MIZUTANI, S. (1970) Silica minerals in the early stage of diagenesis. *Sedimentology*, vol. 15, p. 419–436.

————(1977) Progressive ordering of cristobalitic silica in the early stage of diagenesis. *Contrib. Mineral. Petrol.*, vol.61,p. 129–140.

MORITANI, T. (1967) Uranium-bearing phosphate rocks from the Nanao district of the Noto Peninsula (abstract). *Jour. Japan. Assoc. Mineral. Petrol. Econ. Geol.*, vol. 57, p. 129 (in Japanese).

OGIWARA, S. and TAGUCHI, K. (1986) Some phosphatic nodules from Japan — newly found phosphatic nodules from Japan Sea side region of Northeast Japan (abstract). *Jour.*

*Japan. Assoc. Mineral. Petrol. Econ. Geol.*, vol. 81,p. 155–156 (in Japanese).

ŌTSUKA, S. (1900) On the phosphate in Hyūga Province. *Bull. Imperial Geol. Surv. Japan*, vol. 14, no. 1, p. 1–42 (in Japanese).

PISCIOTTO, K. A. and GARRISON, R. E. (1981) Lithofacies and depositional environments of the Monterey Formation, California. in *The Monterey Formation and Related Siliceous Rocks of California*, Soc. Econ. Paleontol. Mineral., Pacific Section, p. 97–122.

SUGAI, K., MATSUI, H., SATO, S., KITAGAWA, Y., SASAKI, M., MIYASHITA, M. and KAWACHI, H. (1957) *Geological maps of the coal fields of Japan, I. Geological map and explanatory text of Jōban Coal Field.* Geol. Surv. Japan., 143 p. (in Japanese with English abstract).

TSUNETO, N. (1897) Phosphate in Hyūga Province. *Report on the Investigation of Mineral Fertilizer*, no. 1, Imperial Geol. Surv. Japan, 118 p. (in Japanese).

## 常磐炭田勿来付近の前期中新世亀ノ尾層から見いだされた燐酸塩ノジュール

鹿 野 和 彦

### 要　旨

　前期中新世亀ノ尾層の一露頭から見いだされた燐酸塩ノジュールを堆積岩岩石学的に検討した結果について述べた.

　このノジュールは珪藻軟泥起源のポーセラナイト質岩中に産し，$P_2O_5$ を 8–16 wt% 含む. 燐の大部分は apatite(恐らく，carbonate-fluorapatite)として存在し，シリカとの間に逆相関関係が認められる. ノジュールは燐がシリカを交代することによって形成されたものであり，その形成時期はシリカ鉱物の続成変化から続成作用の早期と考えられる.
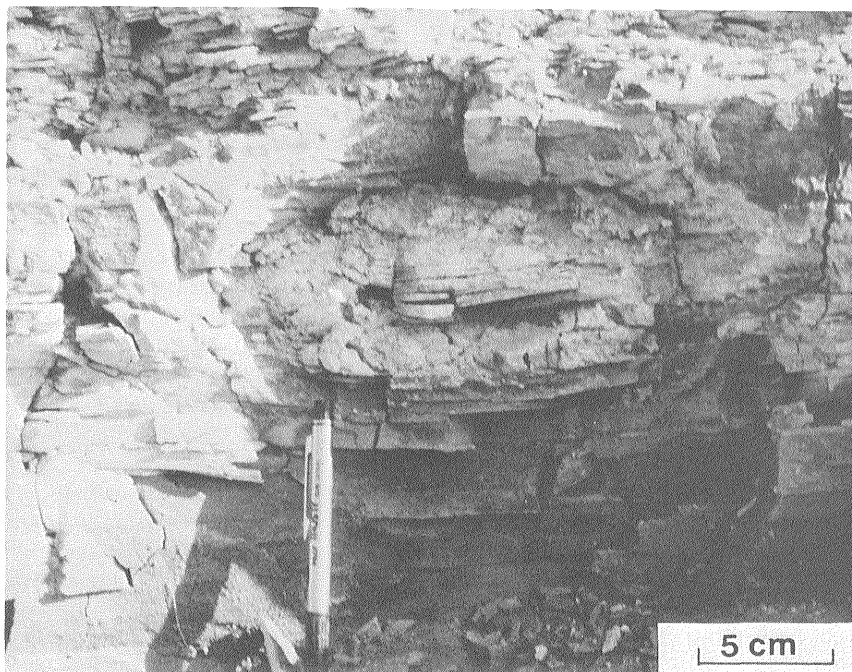
Plate I    Phosphatic nodule in porcellaneous shale. Shale parting can be traced from the porcellaneous shale to the nodule, suggesting the replacement origin of the nodule.

Plate II    Scanning electron micrographs of phosphatic nodule (R33286). Cocoon-shaped or oval grains ⇒ of apatite and opal–CT lepispheres are dominant in the nodule (A and B). A1, A2, A3 and A4 are the energy-dispersive X–ray spectrographs of the grains 1, 2, 3 and 4 in the photograph A, respectively. The spectrographs reveal that the cocoon-shaped or oval grains 1, 2 and 3 are of apatite, and the grain 4 is opal–CT.

*Plate II*